Cancer Research

miR-31 Ablates Expression of the HIF Regulatory Factor FIH to Activate the HIF Pathway in Head and Neck Carcinoma

Chung-Ji Liu[1,3,4], Meng-Miao Tsai[1], Pei-Shih Hung[1], Shou-Yen Kao[1,5], Tsung-Yun Liu[6], Kou-Juey Wu[2], Shih-Hwa Chiou[6], Shu-Chun Lin[1,5], and Kuo-Wei Chang[1,5,6]

Abstract

MicroRNAs (miRNA) are endogenously expressed noncoding RNAs with important biological and pathological functions that are yet to be fully defined. This study investigated alterations in miRNA expression in head and neck squamous cell carcinoma (HNSCC), the incidence of which is rising throughout the world. Initial screening and subsequent analysis identified a panel of aberrantly expressed miRNAs in HNSCC tissues, with *miR-31* among the most markedly upregulated. Ectopic expression of *miR-31* increased the oncogenic potential of HNSCC cells under normoxic conditions in cell culture or tumor xenografts. Conversely, blocking *miR-31* expression reduced the growth of tumor xenografts. The *in silico* analysis suggested that *miR-31* may target the 3′ untranslated region (UTR) of factor-inhibiting hypoxia-inducible factor (FIH), a hypoxia-inducible factor (HIF) regulatory factor that inhibits the ability of HIF to act as a transcriptional regulator under normoxic conditions. In support of this likelihood, *miR-31* expression repressed FIH expression and mutations within the predictive *miR-31* target site in the *FIH* 3′ UTR abrogated FIH repression. Furthermore, *miR-31* expression increased HIF transactivation activity. We found that FIH suppressed oncogenic phenotypes under normoxic conditions and that this activity was abrogated by functional mutations. Lastly, increased *miR-31* expression was correlated with decreased levels of FIH in tumor tissues. Our findings suggest that *miR-31* contributes to the development of HNSCC by impeding FIH to activate HIF under normoxic conditions. *Cancer Res; 70(4); 1635–44. ©2010 AACR.*

Introduction

Head and neck squamous cell carcinoma (HNSCC) is the fifth most common carcinoma worldwide (1, 2). MicroRNAs (miRNA) are 19 to 24 nucleotides noncoding RNAs that regulate the translation and degradation of target mRNAs (3, 4). Lines of evidence indicate that miRNA may play important roles in carcinogenesis (5). The abundance of miRNAs and their apparent pluripotent actions suggest that the identification of miRNAs involved in oncogenesis might yield targets or networks that are suitable for therapeutic intervention (3). *miR-21* was found to be oncogenic in HNSCC (6–8). *miR-98* regulates HMGA2 expression in HNSCC cells (9). An association has also been identified between *miR-211* expression and the vascular invasion of oral carcinoma (10). miRNA expression can also be used as a diagnostic marker of HNSCC (7, 11).

Hypoxia-inducible factor-1α (HIF-1α) and HIF-2α are key transcription factors induced by hypoxia, which activate a transcription program that promotes aggressive tumor phenotypes by triggering the expression of critical genes, including vascular endothelial growth factor (VEGF), TWIST transcription factor, and others (12, 13). When sensing the oxygen tension, asparagine hydroxylation by factor-inhibiting HIF-1α (FIH) inactivates the COOH terminal transactivation domain (C-TAD) region of HIF-1α (14, 15). VEGF is one of the hypoxia-inducible C-TAD–regulated genes (12). FIH is a dioxygenase (14); mutations disrupting the oxygen sensing or the dimerization of FIH molecule resulted in FIH inactivation (16, 17). FIH also modulates other elements and drives diverse phenotypic effects (14, 15). Although FIH expression is associated with neoplastic progression (18–20), the functional role of FIH in tumorigenesis has been obscure.

miR-31 was upregulated in hepatocellular carcinoma (HCC), colorectal carcinoma (CRC), breast carcinoma, and tongue carcinoma (7, 21–24). However, downregulation of *miR-31* or deletion of 9p21 locus harboring pri-*miR-31* was also found in malignancies (25, 26). A recent study showed the upregulation of *miR-31* in metastasis-free breast carcinoma and *miR-31* drives inhibitory effects on breast cancer metastasis by targeting multiple genes (27). In this study, we

Authors' Affiliations: [1]Institute of Oral Biology and [2]Institute of Biochemistry, National Yang-Ming University; [3]MacKay Medicine, Nursing and Management College; [4]Department of Oral and Maxillofacial Surgery, Taipei MacKay Memorial Hospital; [5]Department of Stomatology and [6]Department of Medical Research and Education, Taipei Veterans General Hospital, Taipei, Taiwan

Note: Supplementary data for this article are available at Cancer Research Online (http://cancerres.aacrjournals.org/).

C.J. Liu and M.M. Tsai contributed equally to this work.

Corresponding Author: Kuo-Wei Chang, Department of Dentistry, School of Dentistry, National Yang-Ming University, No. 155, Li-Nong Street, Section 2, Taipei 112, Taiwan. Phone: 886-2-28267223; Fax: 886-2-28264053; E-mail: ckcw@ym.edu.tw or Shu-Chun Lin, Institute of Oral Biology, School of Dentistry, National Yang-Ming University, No. 155, Li-Nong Street, Section 2, Taipei 112, Taiwan. Fax: 886-2-28264053; E-mail: sclin@ym.edu.tw.

doi: 10.1158/0008-5472.CAN-09-2291

identified that *miR-31* transactivated HIF in normoxia and enhanced the oncogenesis of HNSCC via FIH, which acts as a target.

Materials and Methods

HNSCC tissues. Resected tissues from 46 HNSCC patients (Supplementary Table S1), who gave informed consent for the use of their tissue, were harvested at surgery. The study was approved by the institutional review board. Tissue specimens were taken from primary HNSCC, along with paired noncancerous matched tissues (NCMT) as well as available neck metastatic lesions (NML). Ten primary tumor tissues were microscopically screened to have >70% of their areas occupied by tumor cells; these were used to analyze a panel of 154 highly conserved miRNAs using quantitative reverse transcription–PCR (qRT-PCR) array (Applied Biosystems). The results of this assay allowed the selection of particular miRNAs to be assessed in tissues retrieved by laser capture microdissection (LCM; ref. 1).

Quantitative PCR. A *mir*Vana PARIS kit (Ambion) was used to isolate miRNA from the total RNA. A Taqman miRNA assay kit and Taqman miRNA assay supplies were used to quantify the expression of mature miRNAs according to the manufacturer's instructions (Applied Biosystems). miRNA-specific qRT-PCR was done in duplicate or triplicate on the ABI Prism 7700 Sequence Detector system (Applied Biosystems) using *RNU19* or *let-7a* as internal controls (28). C_t was the number of cycle at which the fluorescence signal passed threshold. ΔC_t was the difference of C_t values between tested miRNA and internal control (10). $\Delta\Delta C_t$ was the difference of ΔC_t values between different experimental settings or paired samples. $2^{\Delta\Delta C_t}$ represents the fold change in miRNA expression. mRNA expression of *FIH, ING4*, and *PHD4* was analyzed using Taqman qRT-PCR analysis (Applied Biosystems).

Cell culture, reagents, and phenotypic assays. The HNSCC cell lines Fadu, OECM-1, and SAS cells; HT29 CRC cells; and 293FT and phoenix package cells were cultured as previously described (2, 29), as were normal human oral keratinocytes (NHOK), which were used as controls (30). Fadu and SAS were tumorigenic, whereas OECM-1 was nontumorigenic in nude mice (31). For hypoxia culture, cells were grown in an incubator (Astec) with 1% O_2, 5% CO_2, and 94% N_2 for 24 h. *miR-31* antisense locked nucleic acid (2′-O,4′-C-methylene-linked ribonucleotide derivative; LNA) together with control scramble LNA were purchased from Ambion. The inhibitory efficacy of *miR-31* LNA in cultivated SAS cells was validated as 120 nmol/L for 24 to 72 h. The dose of *miR-21* mimic (Ambion) was determined as 30 nmol/L by pilot studies. VEGF production in aliquots of cell supernatant or tissue lysate was analyzed using a kit (Invitrogen). Analysis of cell viability, proliferation, migration, and anchorage-independent colony formation followed the protocols previously published (2).

Plasmids, transfection, and infection. For exogenous *miR-31* expression, *pre-mir-31* sequence was cloned into a lentivirus vector, pLV-EF1a-GFP, which contains a green fluorescent protein (GFP) tag (10). An empty vector or a vector carrying the *miR-31* insert was cotransfected with helper plasmids into 293FT cells to produce lentiviruses. The stable cell lines were established by lentiviral infection.

To test the targeting activity of *miR-31*, antisense sequences complementary to *miR-31* sequences and the 3′ untranslated region (UTR) of FIH containing predictive *miR-31* target sites were cloned into the pCMV-LacZ plasmid at the 3′-end of the *lacZ* coding sequence; these reporter plasmids were designated *miR-31*-asR and pCMV-LacZ-FIH3′UTR, respectively. Cotransfection of reporter plasmids with pCMV-Luc into cells was performed using Lipofectamine 2000 (Life Technologies). *LacZ* gene expression would be repressed if the *pre-mir-31* insert was expressed, processed, and served as small interfering RNA against *lacZ*. Two putative *miR-31* target sites residing at nucleotides 117 to 124 and 774 to 780 in the FIH3′UTR predicted by TargetScan[7] and Pictar[8] were designated A and B as conservative and nonconservative sites, respectively. Mutant reporter plasmids were obtained from pCMV-LacZ-FIH3′UTR using a site-directed mutagenesis kit (Stratagene). After confirmation of the replacement of the target sequence *UCUUGC* by *AAGCUU*, the plasmids were designated A Mut, B Mut, and AB Mut, which had mutations in A, mutations in B, and double mutations in both A and B sites, respectively.

pHIF1-luc reporter plasmid (Panomics) was used for the assay of HIF transactivation.

For exogenous FIH expression, two wild-type and two mutant FIH cDNA sequences generated by site-directed mutagenesis were cloned into pBabe-puro vector to produce retroviruses for infection. The stable cells FIH(3′UTR), FIHWt, FIHD201A, and FIH 1-302 cells were established by puromycin selection after retroviral infection. FIH(3′UTR) cells would express wild-type full-length *FIH* cDNA, including 3′ UTR, whereas FIHWt would express wild-type *FIH* coding sequence without 3′ UTR. FIH is a dioxygenase, and its activity is Fe(II) dependent (14). FIH D201A cells would express a mutant FIH coding sequence encompassing an aspartic acid-to-alanine mutation at residue 201 that disrupts Fe (II) binding and attenuates catalytic activity. FIH 1-302 cells would express a protein with truncation of 303 to 349 residues that prevents the dimerization of FIH molecules at COOH terminal region and attenuates FIH (16, 17). Vector alone is a control cell infected with control virus.

Western blot analysis. Cell lysate (80 μg), cytosolic fraction (80 μg), and nuclear extract (40 μg) were isolated using previously described protocols (27). Western blot analysis followed previously used protocols (2). The providers and dilution of the primary antibodies are presented in Supplementary Table S2.

Immunohistochemistry. FIH and VEGF immunoreactivities in HNSCC, together with available NCMT and NML, were detected by immunohistochemistry following previously reported protocols (1). Incubation of primary antibodies

[7] http://targetscan.org; v4
[8] http://pictar.mdc

was at 4°C overnight (Supplementary Table S2). Preimmunized mouse IgG was used as a negative control. The immunoreactivity was scored −, +, and ++ when <10%, 10% to 50%, and >50% immunoreactive cells were counted, respectively, in five randomly selected 200× fields.

Tumorigenesis. The analysis of tumorigenesis followed the previously published protocols (10). For blockage of xenographic tumors, 0.5% atelocollagen (Koken Co.) on pepsin treatment to remove antigenecity was complexed with 2.5 μmol/L *miR-31* LNA and equivalent scramble controls in a volume of 200 μL. When SAS xenografts grow to ~0.2 cm^3, the complexes were injected s.c. to the periphery of tumors (31).

Statistical and bioinformatics analysis. Pair-wise analysis was performed using website-accessible Generalized Association Plots (GAP) program.[9] Mann-Whitney test and Fisher's exact test were used to compare the differences among variants. Receiver operating characteristic (ROC) analysis was performed, and the area under curve was used as a measurement for the level of separation between clinical settings. The leave-one-out cross-validation (LOOCV) model was used to compute the accuracy of assays. A P value of <0.05 was considered statistically significant.

Results

Upregulation of miR-31 in HNSCC. The miRNA expression profile of HNSCC was achieved from 10 screened tumors analyzed with qRT-PCR array (Supplementary Table S3). miRNAs having concordant $\Delta\Delta C_t$ of >0 or <0 across at least seven screened tumors relative to their paired NCMT were selected for further stratification. The average $\Delta\Delta C_t$ was >1 for 22 miRNAs and <−1 for 9 miRNAs. These miRNAs were therefore considered aberrant in the HNSCC samples (Fig. 1A). Six tumors had high correlation in the miRNA aberration. The highest overexpression was found for *miR-31*, and *miR*-21 was also markedly upregulated. GAP analysis showed a strong correlation between expression of *miR-31* and *miR-21, miR-34b* and *miR-34c*, and *miR-99a* and *miR-100* (Fig. 1B). Analysis of the 46 LCM-retrieved samples confirmed that there was an increase in *miR-21, miR-31*, and *miR-371* in 89%, 84%, and 70% HNSCC relative to NCMT, respectively (Fig. 1C). *miR-31* was confirmed to be shown the greatest level of overexpression in HNSCC, with a mean $\Delta\Delta C_t$ of 3.64. ROC and LOOCV analyses indicated the analytic power (0.82) and accuracy (0.72) using *miR-31* expression to dissect NCMT from HNSCC (Fig. 1D). The analytic power was better than that shown by *miR-21* expression or *miR-371* expression (Supplementary Fig. S1). No significant association was identified between *miR-31* expression and clinical parameters.

miR-31 expression increased the oncogenic potential of HNSCC cells. HNSCC cells had higher *miR-31* expression relative to NHOK (Supplementary Fig. S2). Blockage of *miR-31* expression with *miR-31* LNA treatment significantly decreased viability and migration of SAS cells (Fig. 2A). HNSCC cells were infected with lentivirus carrying *miR-31*. The detection of green fluorescence in SAS cells measured infectivity successfully (Fig. 2B, left). SAS-*miR-31* cells exhibited upregulation of *miR-31* expression by 32-fold relative to SAS-GFP control cells. There was also a remarkable Lac Z repression in SAS-*miR-31* cells when transfected with the reporter plasmids *miR-31*-asR (Fig. 2B, right). This suggests the presence of targeting activity in exogenous *miR-31*. SAS-*miR-31* had significantly greater proliferation, migration, and anchorage-independent growth than controls (Fig. 2C). SAS-*miR-31* also showed significantly greater xenographic tumor growth than controls in nude mice (Fig. 2D, left). With the treatment of *miR-31* LNA and atelocollagen mixture (32), the tumorigenic potential of SAS cells was attenuated (Fig. 2D, right).

OECM-1-*miR-31* cells exhibited green fluorescence; upregulation of *miR-31* expression for 10-fold; *miR-31* targeting activity; and increased proliferation, migration, and anchorage-independent growth than OECM-1-GFP control cells. OECM-1-*miR-31* cells exhibited a slight increase in tumorigenicity; however, the difference was not statistically significant (Supplementary Fig. S3A–F). Fadu-*miR-31* cells exhibited a drastically higher tumorigenicity than Fadu-GFP control cells. Blood vessels with a greater diameter were present in Fadu-*miR-31* xenografts than in the controls (Supplementary Fig. S4).

miR-31 targets FIH. TargetScan and/or Pictar systems predicted hypoxia-associated genes *FIH, HIF-3α, ING4*, and *PHD4*, to be putative targets of *miR-31*. Downregulation of *FIH* mRNA expression and protein expression was found in SAS-*miR-31* cells compared with controls. Conversely, upregulation of *FIH* mRNA expression and protein by ~50% on *miR-31* LNA treatment relative to controls was found (Fig. 3A). Preliminary assays excluded *HIF-3α, ING4*, and *PHD4* as *miR-31* targets (Supplementary Fig. S5). To prove the repression of FIH by *miR-31*, the pCMV-LacZ-FIH3′UTR reporter was used. LacZ activity was repressed more in SAS-*miR-31* than in controls; however, the repression reverted on treatment with *miR-31* LNA (Fig. 3B). Conservative and nonconservative predicted targets for *miR-31* in the 3′ UTR of *FIH* was designated as the A site and the B site, respectively. The mutant reporter plasmids A Mut, B Mut, and AB Mut were generated. In SAS-*miR-31* cells, the A site mutation resulted in a considerable reversion of the Lac Z repression compared with the B site mutation (Fig. 3C). Mutations in both A and B sites resulted in a complete reversion of LacZ repression. These findings suggest that the binding of *miR-31* to the conservative site in 3′ UTR may repress FIH expression. For exogenous FIH expression, SAS-*miR-31* cells and SAS-GFP cells were further infected with retroviruses to achieve FIH(3′UTR) and FIHWt subclones. The former expressed *FIH* coding sequence together with 3′ UTR, and the latter expressed only *FIH* coding sequence. These subclones exhibited an increase in FIH expression relative to control subclones (Fig. 3D, top). The FIH expression in FIH (3′UTR) and FIHWt subclones from SAS-*miR-31* cells was lower than corresponding subclones from SAS-GFP cells. Similar changes were also present in OECM-1 cells (Supplementary Fig. S3H). Furthermore, FIH expression is higher in

[9] http://gap.stst.sinica.edu.tw

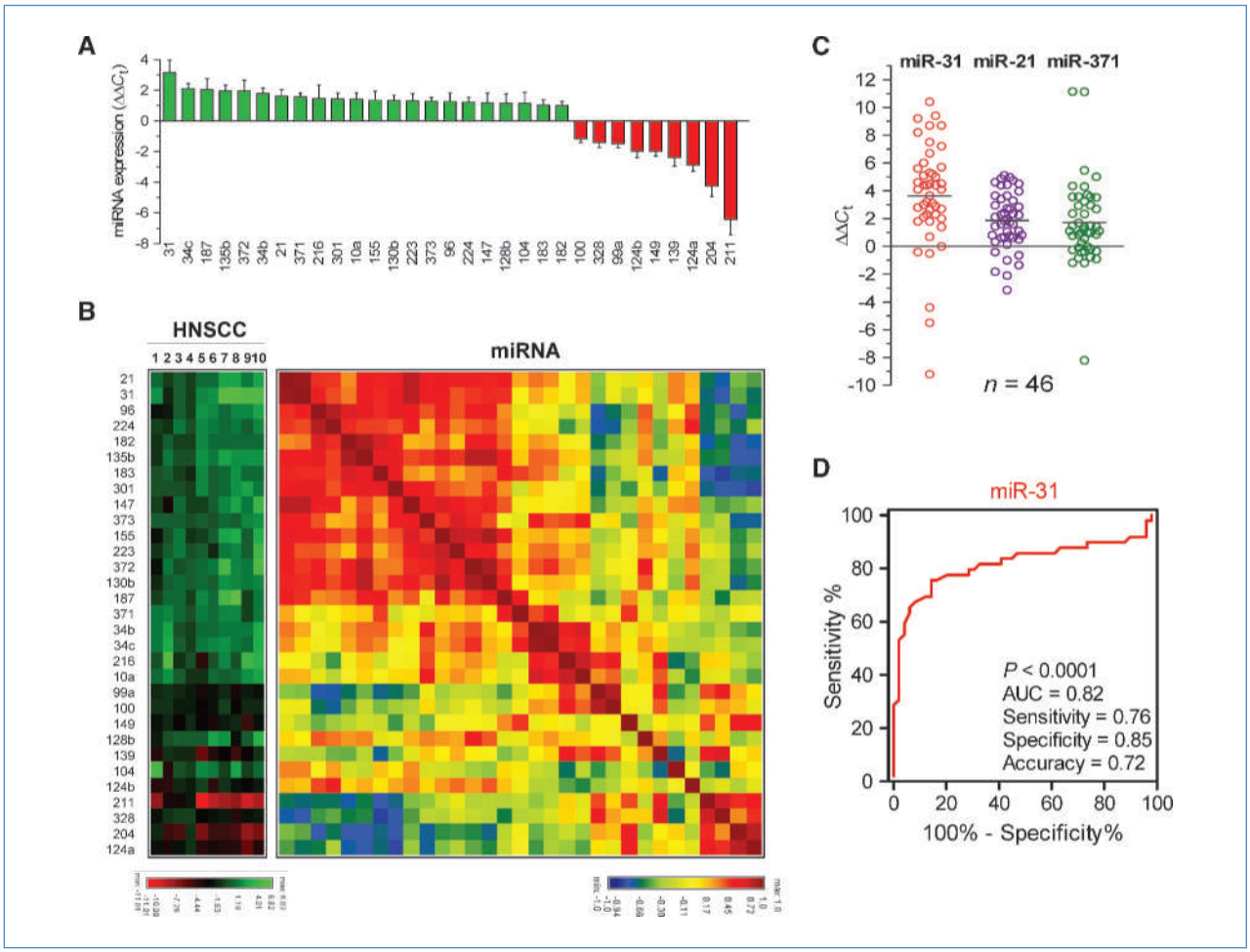

Figure 1. miRNA expression profile. A, 31 differentially expressed miRNAs with an average $\Delta\Delta C_t$ of >1 or <–1 in tumor cells compared with normal tissue. Mean ± SEM of the $\Delta\Delta C_t$ from 10 screened tumor tissues. Green, upregulated; red, downregulated. B, GAP analysis. Left, unsupervised hierarchical algorithm of miRNA expression of patients; right, association plot analysis using miRNA expression profile indicated an association of expression profile in several clusters of miRNA marked by dark red. C, scatter dot plot of the expression of *miR-31, miR-21*, and *miR-371* in 46 LCM-retrieved tissues. Horizontal lines, mean values. D, ROC and LOOCV analysis of *miR-31*. It revealed a sensitivity of 0.76 and a specificity of 0.85 using *miR-31* expression to distinguish NCMT from HNSCC.

FIHWt subclones than FIH(3′UTR) subclones in both SAS-*miR-31* cells and OECM-1-*miR-31* cells (Fig. 3D, bottom). These findings validated the presence of a *miR-31* target in the 3′UTR of *FIH*. Sequence complimentarity was found between *miR-21* and *FIH* 3′ UTR using RNA22[10] program. The treatment with *miR-21* mimic upregulated *miR-21* expression and slightly repressed the FIH expression in SAS and OECM-1 cells (Supplementary Fig. S6).

FIH expression decreased the oncogenic potential of HNSCC cells in normoxia. Exogenous FIH expression was associated with decreased proliferation, migration, and anchorage-independent colony formation of SAS-GFP cells under normoxia culture conditions, but not in hypoxia culture (Fig. 4A). Exogenous FIH expression and hypoxia culture had only limited influence on the growth, but exogenous FIH expression significantly decreased migration and anchorage-independent colony formation of OECM-1-GFP cells in normoxia culture (Supplementary Fig. S3I–K). In hypoxic culture, the suppressive function of FIH(3′UTR) was remarkably attenuated. Because FIH function seemed inactivated in the hypoxia state, FIH D201A mutant subcone and FIH 1-302 truncaton subclone were established in SAS cells to insight the effects of FIH activity in normoxia (16, 17). The expression of the exogenous mutant FIH and the truncated FIH was shown by Western blot analysis (Fig. 4B). The suppressive effect of wild-type FIH on anchorage-independent growth (Fig. 4C) and tumorigenesis (Fig. 4D) was significantly reversed by the mutation or the truncation. Thus, FIH activity is suppressive to SAS cells in normoxia.

miR-31 transactivated HIF activity in normoxia. Under normoxia, SAS-*miR-31* cells and OECM-1-*miR-31* cells exhibited a HIF-1α and HIF-2α expression level that is equal to the

[10] http://cbcsrv.watson.ibm.com/rna22

controls (Fig. 5A, top). SAS-GFP cells carrying exogenous FIH variants also had similar levels of HIF-1α and HIF-2α expression. SAS-*miR-31* had higher HIF transactivation activity than controls, and this could be decreased by *miR-31* LNA (Fig. 5A, bottom). The expression of HIF-1α and transactivation of HIF activity in SAS-*miR-31* and controls were induced under hypoxia culture (Fig. 5B, top); however, exogenous *miR-31* expression had no effect on HIF activation in hypoxia (Fig. 5B, bottom). In normoxia, SAS-*miR-31* showed higher proliferation, migration, and anchorage-independent growth than controls, but this was not the case in hypoxia culture (Fig. 5C, a–c). VEGF production in SAS-*miR-31* was higher than in the controls during normoxia, but VEGF production in SAS-*miR-31* and the controls were similar under hypoxia (Fig. 5C, d). VEGF production in OECM-1-*miR-31* was also higher than control cells during normoxia (Supplementary Fig. S2G). SAS-*miR-31* xenografts showed higher VEGF production than SAS-GFP tumors, whereas SAS xenografts carrying exogenous FIH expression showed lower VEGF production (Fig. 5D).

Exogenous miR-31 expression decreased both cytosolic and nuclear FIH in SAS cells. Exogenous FIH expression resulted in a greater increase in cytosolic FIH compared with nuclear FIH; and exogenous *miR-31* expression seemed to decrease nuclear FIH more remarkably than cytosolic FIH in SAS cells (Supplementary Fig. S7). Exogenous *miR-31* decreased FIH expression and exogenous FIH increased FIH expression in SAS xenografs (Supplementary Fig. S8).

Decreased FIH and increased VEGF during head and neck carcinogenesis. FIH immunoreactivity was detected in the lower half of the epithelium in NCMT. This displayed heterogeneity in terms of cellular localization including the cytosol, membrane, and nucleus (Fig. 6A, a, b and B, a). Intensive cytosolic FIH was found in all HNSCC (Fig. 6A, a, c and B, a, b). In tissue pairs available for comparison, the FIH immunoreactivity was remarkably attenuated in the NML in relation to their HNSCC counterparts (Fig. 6B, b, c). A statistically significant difference in FIH immunoreactivity was found between HNSCC and NML (Supplementary

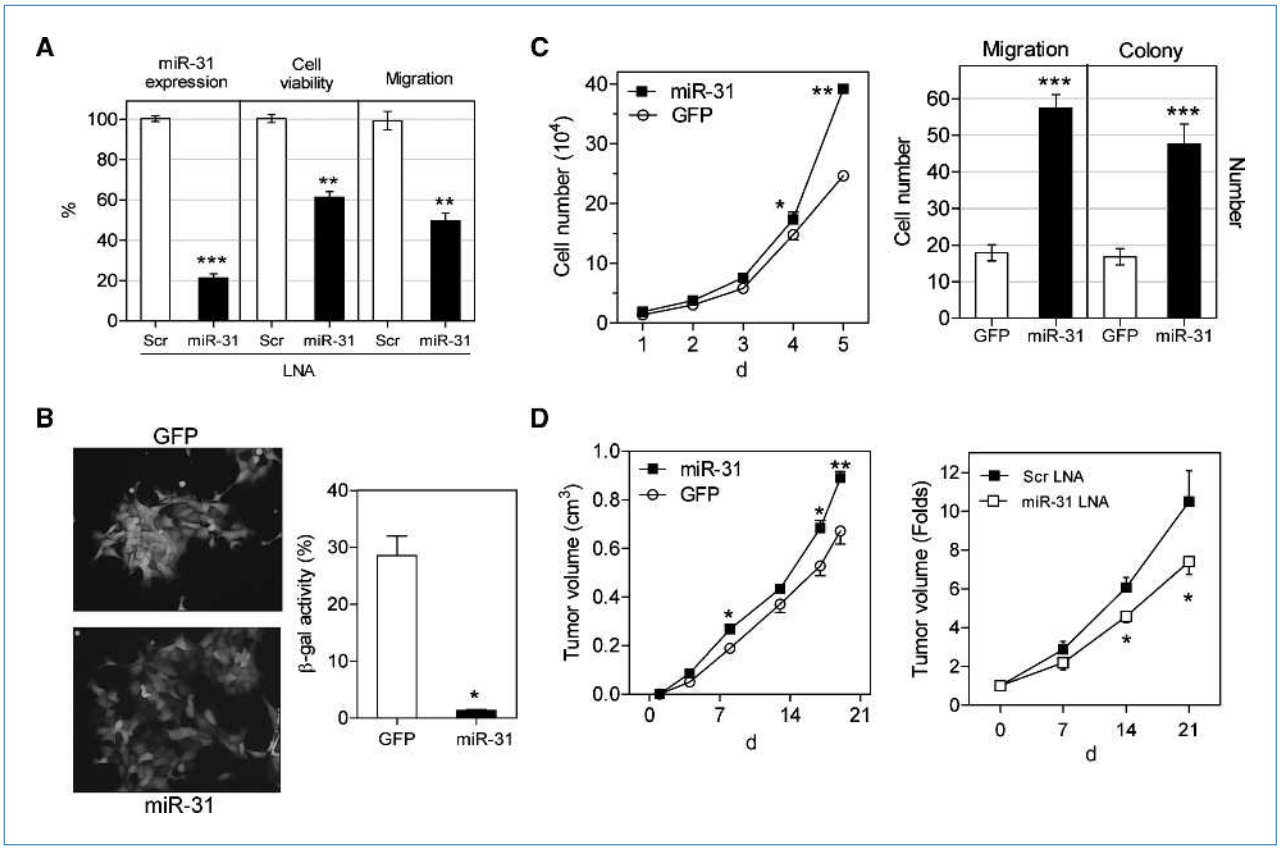

Figure 2. Phenotypic effect of *miR-31*. A, blockage of *miR-31* in SAS cells. *miR-31* expression was decreased with *miR-31* LNA treatment for 24 h. The treatment for 48 h also decreased cell viability and migration. B, left, green fluorescence in SAS-*miR-31* cells and SAS-GFP cells; right, reporter assay. It showed the targeting of *miR-31* to antisense sequence in reporter plasmid *miR-31*-asR, which resulted in a repression of β-galactosidase activity in SAS-*miR-31* cells compared with controls. C, exogenous *miR-31* expression increased proliferation (left), migration, and anchorage-independent colony formation (right) in SAS cells. D, tumorigenesis. Exogenous *miR-31* expression increased the growth of SAS xenografts (left), whereas the blockage of endogenous *miR-31* expression using *miR-31* LNA complexed with atelocollagen decreased the tumorigenic potential of SAS cells (right). Mean ± SEM from triplicate or quadruplicate analysis or from at least five mice. *, $P < 0.05$; **, $P < 0.01$; ***, $P < 0.001$; Mann-Whitney analysis.

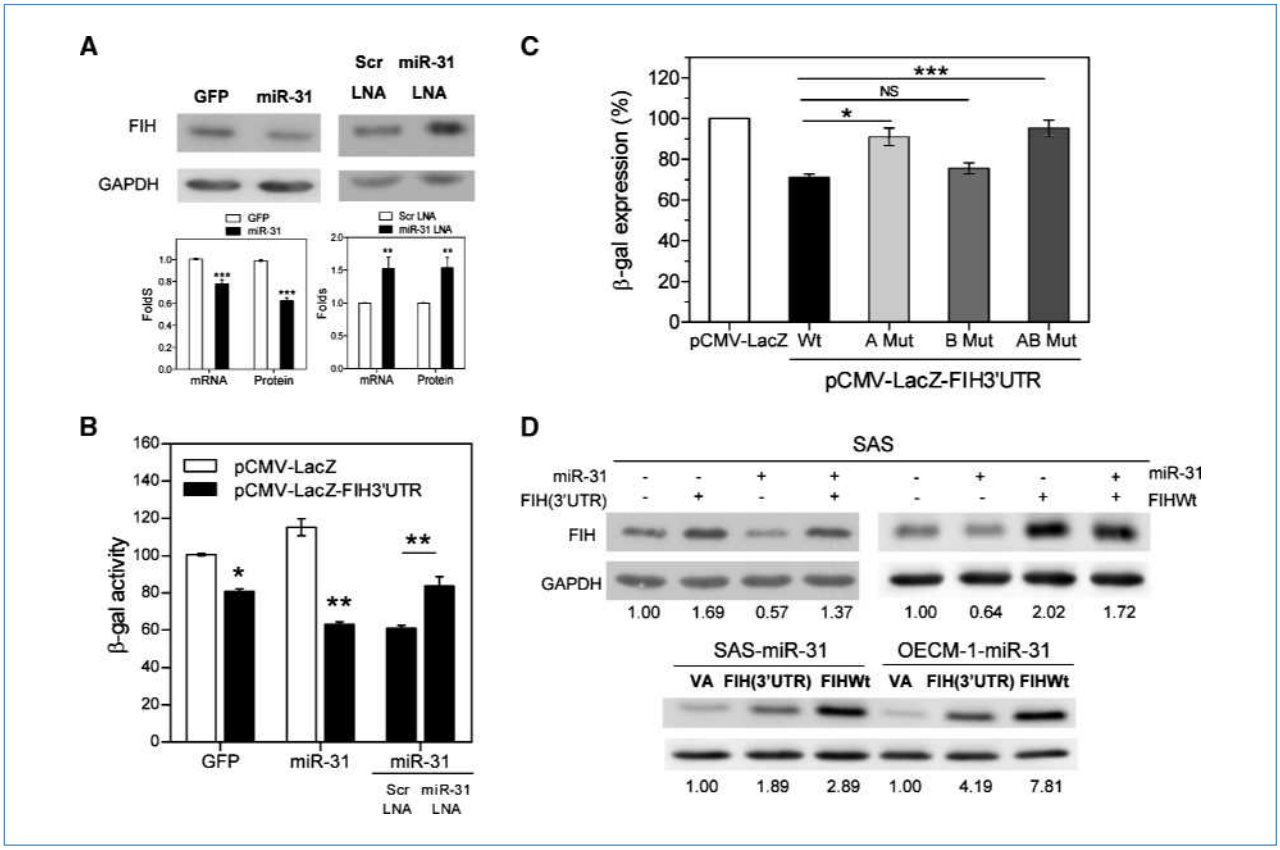

Figure 3. *miR-31* targets FIH. A, FIH expression in SAS cells with exogenous *miR-31* expression or after treatment with *miR-31* LNA. Top, Western blot analysis; bottom, quantification of *FIH* mRNA expression and FIH protein expression. B and C, reporter assays. B, SAS-*miR-31* cells transfected with reporter plasmid pCMV-LacZ-FIH3′UTR exhibited a remarkable decrease in β-galactosidase activity comparing with controls. The repression was reverted after treatment with *miR-31* LNA. C, SAS-*miR-31* cells were transfected with pCMV-LacZ-FIH3′UTR and mutant reporters. The repression of β-galactosidase activity was not seen after transfection with A Mut and AB Mut. The results suggested that the A sequence may be the crucial *miR-31* target of FIH. Mean ± SEM from triplicate or quadruplicate analysis. *, $P < 0.05$; **, $P < 0.01$; ***, $P < 0.001$. NS, not significant. Mann-Whitney analysis. D, Western blot analysis of FIH expression in various subclones. Numbers below the figures are the normalized FIH expression values.

Table S4). Nuclear FIH was obvious in the superbasal cell layer of the NCMT samples, and it seemed stronger than the cytosolic FIH (indent in Fig. 6A, d). Only 24% of HNSCC samples were scored as having nuclear FIH immunoreactivity in >10% cells. A statistically significant decrease in nuclear FIH from NCMT samples to HNSCC samples was noted (Supplementary Table S4). A reverse association lying between *miR-31* expression and nuclear FIH immunoreactivity was also noted in HNSCC (Supplementary Table S5).

There was 18% NCMT (Fig. 6C, a) and >60% HNSCC (Fig. 6C, b) or NML (Fig. 6C, c) having cytosolic VEGF immunoreactivity in >50% cells. A statistically significant increase of VEGF immunoreactivity from NCMT to HNSCC was noted (Supplementary Table S6). A trend for reverse association lying between nuclear FIH immunoreactivity and VEGF immunoreactivity was found in HNSCC samples. A reverse association lying between nuclear FIH immunoreactivity and VEGF immunoreactivity was noted in NML and the overall tumor tissues consisting of HNSCC and NML (Supplementary Table S7).

Discussion

We identified significant upregulation of *miR-31* in HNSCC tumors and cell lines, which is similar to the situation with several important human cancers (7, 21–24). However, only expression studies were carried out during the above research, and no study up to the present has ever addressed the regulation and function of *miR-31* in HNSCC, CRC, or HCC (7, 21–24). Our functional characterization verified the oncogenic roles of *miR-31* in HNSCC, and this result was supported by the enhancement of *in vitro* oncogenicity and tumorigenesis after overexpression in cell lines. The oncogenic roles of *miR-31* were also substantiated by *in vitro* or *in vivo* clues from *miR-31* blockage. It seems that the increase in tumor induction was limited when *miR-31* was overexpressed in SAS and OECM-1 cells. Because the endogenous expression of *miR-31* has been found to be high in HNSCC tissues and cells, the exogenously expressed *miR-31* might allow only limited further enhancement of tumor growth. We provide evidence that the oncogenic potential of *miR-31* is abrogated

in hypoxia status. As a consequence, SAS or OECM-1 xenografts are postulated to contain a high fraction of hypoxic cells and limited *miR-31* functionality. Our study also confirmed the upregulation of *miR-21* and *miR-371* in HNSCC (6–8). Although the dissection power of *miR-21* expression did not exceed that of *miR-31* in distinguishing benign from malignant status, *miR-21* should still play key roles in HNSCC and other malignancies, because it targets crucial suppressors (4, 5, 8, 33).

Hypoxia is linked to epithelial-mesenchymal transition, metastasis, and therapy resistance among neoplasms (12). Using blockers, an exogenous expression system, reporters, and mutant constructs, we were able to verify that *miR-31* targets the conservative complementary sequence in the 3′ UTR of FIH and transactivates HIF under normoxia. This resulted in an increase in VEGF and other factors that could be contributive to the HNSCC pathogenesis (11, 12). Although *miR-17-92* cluster and *miR-210* were shown involved in the regulation of hypoxia (34–36), this is the first study that identifies a miRNA, which is overexpressed in HNSCC, as being involved in the indirect activation of HIF through targeting FIH during normoxia. Several HNSCCs were found to have extremely low *miR-31* expression. Loss of heterozygosity at 9p21 frequently altered in HNSCC could be the underlying genomic event (37). Preliminary analyses showed that *miR-21* repressed FIH, whereas further analyses are required to clarify FIH as a target of *miR-21*. Because *miR-21* expression was correlated with *miR-31* expression in HNSCC, their synergistism for HNSCC development should be unraveled. It was known that HIF activation occurs during hypoxia and that this usually occurs at a late stage of neoplastic process. Because the downregulation of *miR-31* occurs in metastatic breast carcinoma (27) and tumor metastasis occurs mainly in deeper tissue regions probably having oxygen deficiency (38), wherein *miR-31* could be unable to activate HIF to augment the aggressiveness of HNSCC, different mechanisms regulated by FIH in hypoxic tumor regions must be further investigated. Whether *miR-21* plays more prominent roles for HNSCC metastasis than *miR-31* is also an interesting issue to be addressed (8).

FIH suppressed HNSCC during normoxia, and the suppression was abrogated in hypoxic culture. The findings were concordant with the fact that *miR-31* enhanced oncogenicity only when oxygen supply is sufficient. This study also provided functional clues by inactivating FIH using mutant constructs, which specified the requirement of FIH activity for

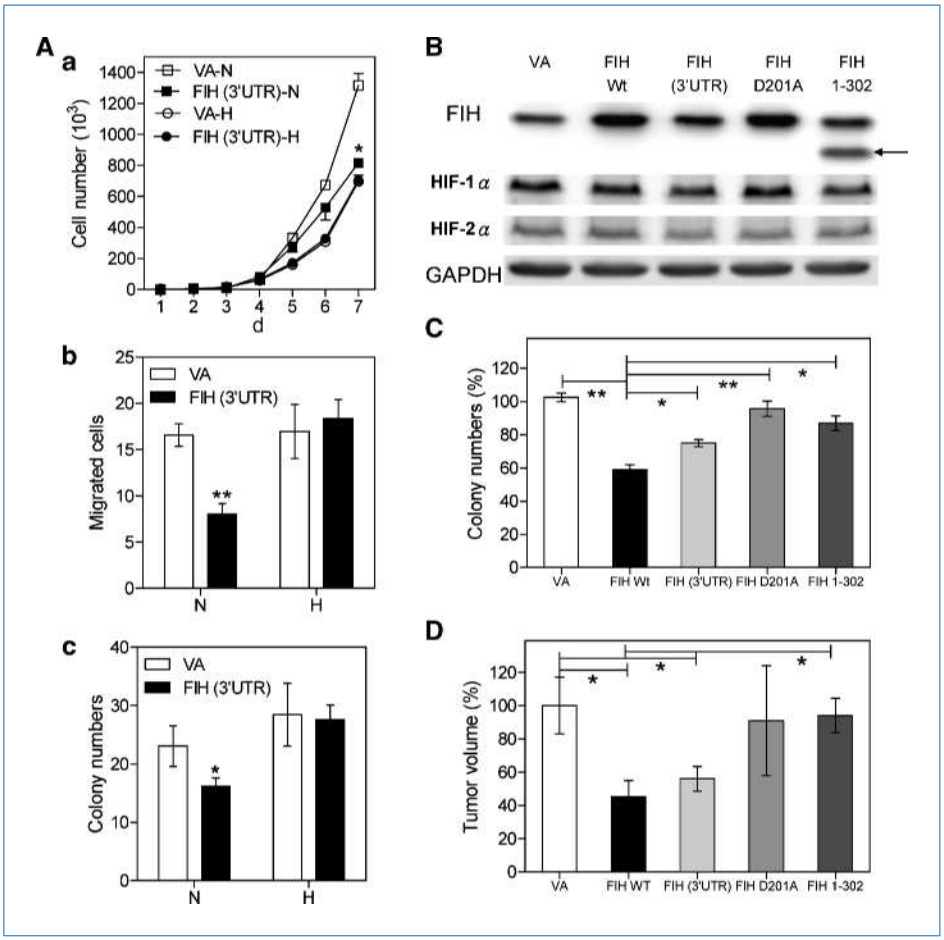

Figure 4. FIH suppresses the oncogenicity in normoxia. A, the phenotypes of SAS cells. a-c, assays for proliferation, migration, and anchorage-independent colony formation, respectively. N, normoxia; H, hypoxia. B-D, SAS-GFP cells. B, Western blots analysis of FIH expression in various subclones. An arrow indicates the truncated FIH. C and D, anchorage-independent colony formation and tumorigenesis, respectively, for various subclones. Mean ± SEM from triplicate or quadruplicate analysis or five nude mice. *, $P < 0.05$; **, $P < 0.01$. Mann-Whitney analysis.

the tumor suppression in normoxia (16, 17). Nuclear FIH was prominent in the superbasal layers of NCMT, whereas it was significantly decreased in HNSCC. Nuclear FIH expression was opposite to the *miR-31* expression in HNSCC. Moreover, a reverse association between nuclear FIH expression and VEGF expression was also found in tumor tissues. These lines of tissue evidence together with the functional clues provided above indicated a *miR-31*-FIH-HIF cascade involved in HNSCC development in normoxia state. Because a reverse association between nuclear FIH expression and VEGF expression was also noted in metastatic lesions, it suggested that the oxygen level in these tissues could be sufficient for nuclear FIH to hydroxylate HIF. The high abundance of FIH protein, particularly cytosolic FIH, was found in HNSCC tissues and cell lines and in other types of cancers (39). In HNSCC cells with exogenous FIH expression, the FIH is localized mainly in cytosol with only a small fraction of the FIH being distributed to the nucleus or onto the membrane (40). In addition, the high cytosolic FIH levels seem to define a poor prognosis or progression for breast carcinoma, non–small cell lung carcinoma, and pancreatic endocrine tumors (18–20). The high abundance of FIH in the cytosol of HNSCC cells might act as a reservoir and allows it to act as a direct oxygen sensor. Alternatively, because FIH also modulates Notch and IκBα by hydroxylation (14, 15, 39, 40), the stability or activity of Notch and IκBα being regulated by cytosolic FIH for pathogenesis requires further stratification using specific constructs.

This study identified that *miR-31* contributes to HNSCC development through HIF activation in tumor regions,

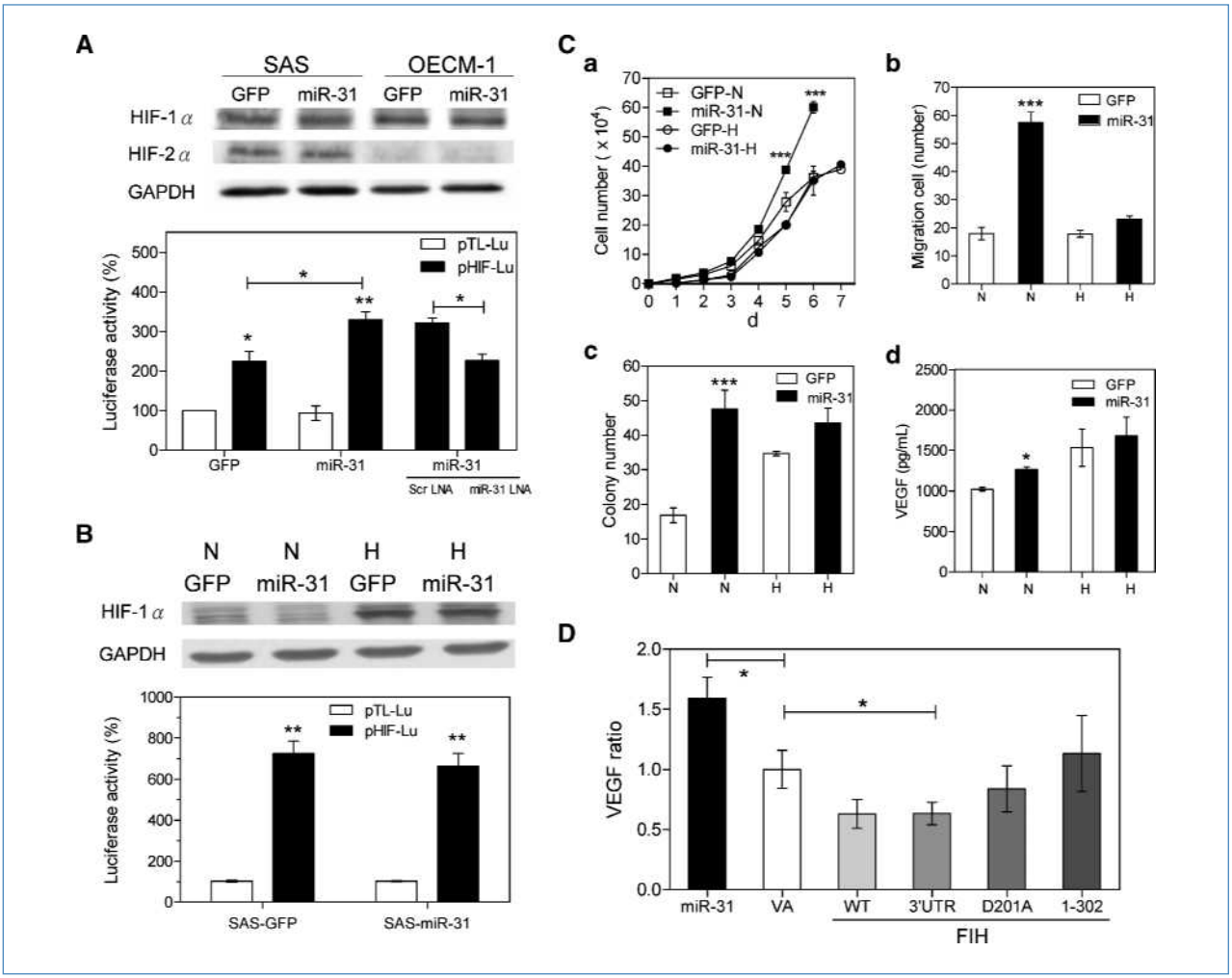

Figure 5. *miR-31* transactivates HIF. A, top, Western blot analysis of HIF-1α and HIF-2α expression in normoxia; bottom, HIF transactivation assay. Exogenous *miR-31* expression resulted in an increase in the transactivation activity of HIF, which is reduced after *miR-31* LNA treatment. B, top, Western blot analysis of HIF-1α. Hypoxia culture induces HIF-1α expression in SAS cells. Bottom, HIF activity during hypoxia culture. Exogenous *miR-31* expression did not change the HIF activity in SAS cells under hypoxia culture. C, SAS cells. a-d, assays for proliferation, migration, anchorage-independent colony formation, and VEGF production at 48 h, respectively. N, normoxia; H, hypoxia. D, VEGF in SAS xenografts. Mean ± SEM from triplicate or quadruplicate analysis or three to four nude mice. *, $P < 0.05$; **, $P < 0.01$; ***, $P < 0.001$. Mann-Whitney analysis.

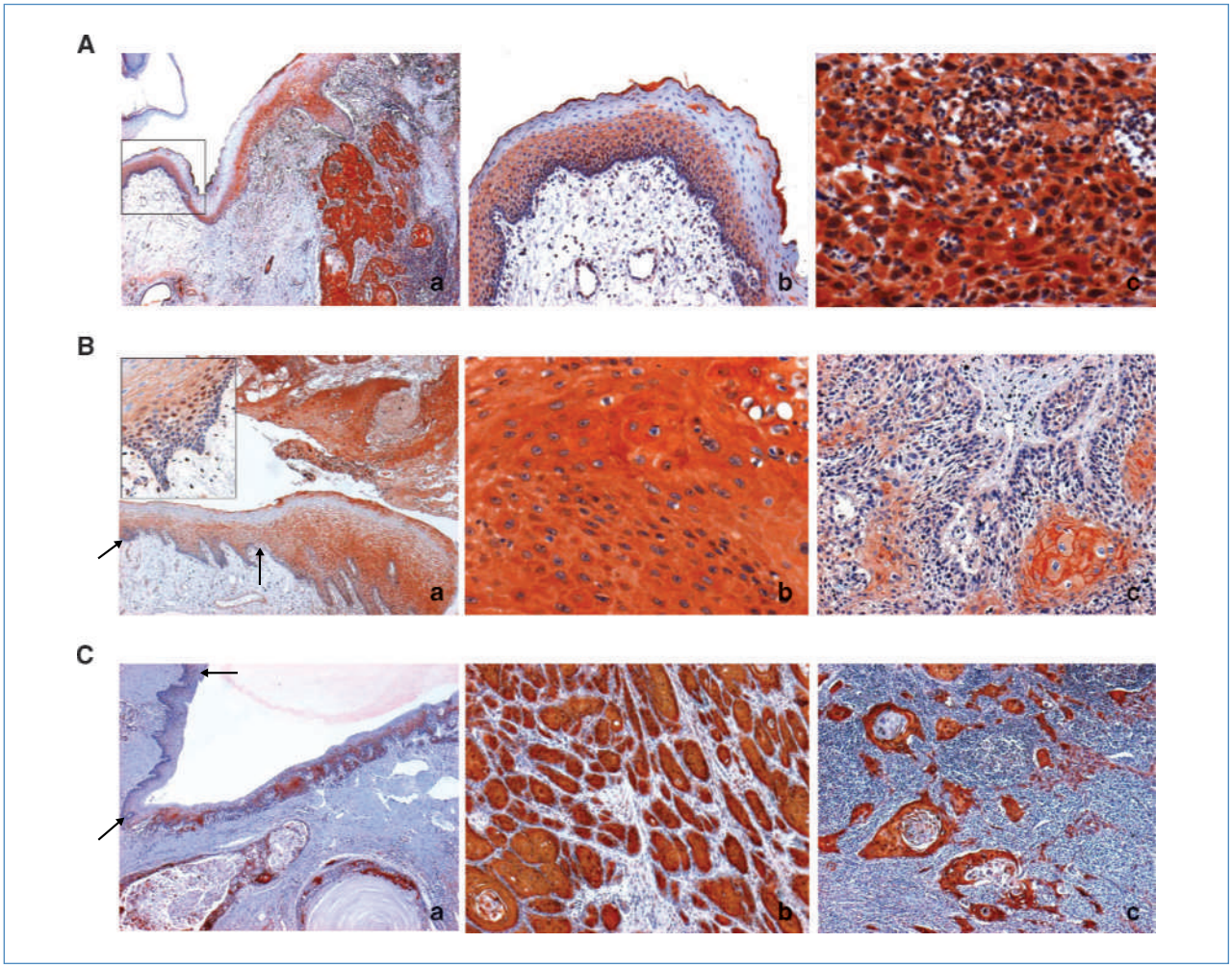

Figure 6. FIH and VEGF immunoreactivity in HNSCC tissues. A and B, FIH; C, VEGF. Red staining is the immunoreactivity. Nuclei are stained blue. A, a representative nonmetastatic HNSCC having *miR-31* expression less than the mean. a, HNSCC tissue and corresponding NCMT (marked by block); b, the amplified picture of a; c, HNSCC. The tumor has both cytosolic and nucleic FIH immunoreactivity. B, a representative metastatic HNSCC having *miR-31* expression greater than the mean. a, HNSCC and NCMT (tissue between arrows); b, HNSCC; c, NML. Indent in a, an amplified portion of NCMT. The HNSCC has only cytosolic FIH immunoreactivity. A drastic decrease in FIH immunoreactivity is noted in NML comparing with HNSCC. Note the cytosolic, membranous, and nucleic FIH immunoreactivity in the lower half of NCMT (A, a, b and B, a). C, a representative HNSCC having high cytosolic VEGF immunoreactivity in HNSCC (b) and corresponding NML (c). The corresponding NCMT (tissue between arrows) was negative for VEGF immunoreactivity, whereas the other dysplastic covering epithelium and tumor portion exhibited VEGF immunoreactivity (a). A, a; B, a; C, ×25; A, b; B, c, ×100; A, c; B, b, ×200.

wherein oxygen level are above the threshold for FIH activity. *miR-31* expression was known to repress several target genes to inhibit the metastasis of breast carcinomas (27); thereby, the identification of other *miR-31* targets and pluripotent actions of *miR-31* involved in different neoplastic stage of tumorigenesis will be important. Further understanding of the pathogenetic significance of other aberrantly expressed miRNAs identified in this study may eventually contribute to diagnosis and interception of HNSCC (11).

Disclosure of Potential Conflicts of Interest

No potential conflicts of interest were disclosed.

Acknowledgments

We thank Dr. Hsi-Feng Tu, Dr. Wen-Yuan Hu, and Hui-Wen Cheng.

Grant Support

National Science Council grants NSC96-2628-B-010-033-MY3, 96-3111-B-075-001-MY3, and 96-2314-B-195-018-MY3, Taipei Mackay Hospital grant 9117, Aim for the Top University Plan from Department of Education grant, and Taipei Veterans General Hospital grant V97ER2-015.

The costs of publication of this article were defrayed in part by the payment of page charges. This article must therefore be hereby marked *advertisement* in accordance with 18 U.S.C. Section 1734 solely to indicate this fact.

Received 6/26/09; revised 10/27/09; accepted 12/7/09; published OnlineFirst 2/9/10.

References

1. Liu CJ, Lin SC, Chen YJ, Chang KM, Chang KW. Array-comparative genomic hybridization to detect genomewide changes in microdissected primary and metastatic oral squamous cell carcinomas. Mol Carcinog 2006;45:721–31.
2. Shieh TM, Lin SC, Liu CJ, Chang SS, Ku TH, Chang KW. Association of expression aberrances and genetic polymorphisms of lysyl oxidase with areca-associated oral tumorigenesis. Clin Cancer Res 2007;13:4378–85.
3. Bartel DP. MicroRNAs: target recognition and regulatory functions. Cell 2009;136:215–33.
4. Dalmay T, Edwards DR. MicroRNAs and the hallmarks of cancer. Oncogene 2006;25:6170–5.
5. Dalmay T. MicroRNAs and cancer. J Intern Med 2008;263:366–75.
6. Chang SS, Jiang WW, Smith I, et al. MicroRNA alterations in head and neck squamous cell carcinoma. Int J Cancer 2008;123:2791–7.
7. Wong TS, Liu XB, Wong BY, Ng RW, Yuen AP, Wei WI. Mature miR-184 as potential oncogenic microRNA of squamous cell carcinoma of tongue. Clin Cancer Res 2008;14:2588–92.
8. Li J, Huang H, Sun L, et al. MiR-21 indicates poor prognosis in tongue squamous cell carcinomas as an apoptosis inhibitor. Clin Cancer Res 2009.
9. Hebert C, Norris K, Scheper MA, Nikitakis N, Sauk JJ. High mobility group A2 is a target for miRNA-98 in head and neck squamous cell carcinoma. Mol Cancer 2007;6:5.
10. Chang KW, Liu CJ, Chu TH, et al. Association between high miR-211 microRNA expression and the poor prognosis of oral carcinoma. J Dent Res 2008;87:1063–8.
11. Avissar M, Christensen BC, Kelsey KT, Marsit CJ. MicroRNA expression ratio is predictive of head and neck squamous cell carcinoma. Clin Cancer Res 2009;15:2850–5.
12. Yang MH, Wu MZ, Chiou SH, et al. Direct regulation of TWIST by HIF-1α promotes metastasis. Nat Cell Biol 2008;10:295–305.
13. Dayan F, Roux D, Brahimi-Horn MC, Pouyssegur J, Mazure NM. The oxygen sensor factor-inhibiting hypoxia-inducible factor-1 controls expression of distinct genes through the bifunctional transcriptional character of hypoxia-inducible factor-1α. Cancer Res 2006;66:3688–98.
14. Cockman ME, Lancaster DE, Stolze IP, et al. Posttranslational hydroxylation of ankyrin repeats in IκB proteins by the hypoxia-inducible factor (HIF) asparaginyl hydroxylase, factor inhibiting HIF (FIH). Proc Natl Acad Sci U S A 2006;103:14767–72.
15. Coleman ML, McDonough MA, Hewitson KS, et al. Asparaginyl hydroxylation of the Notch ankyrin repeat domain by factor inhibiting hypoxia-inducible factor. J Biol Chem 2007;282:24027–38.
16. Dann CE III, Bruick RK, Deisenhofer J. Structure of factor-inhibiting hypoxia-inducible factor 1: an asparaginyl hydroxylase involved in the hypoxic response pathway. Proc Natl Acad Sci U S A 2002;99:15351–6.
17. Hewitson KS, Holmes SL, Ehrismann D, et al. Evidence that two enzyme derived histidine ligands are sufficient for iron binding and catalysis by factor inhibiting HIF (FIH). J Biol Chem 2008;383:25971–8.
18. Couvelard A, Deschamps L, Rebours V, et al. Overexpression of the oxygen sensors PHD-1, PHD-2, PHD-3, and FIH is associated with tumor aggressiveness in pancreatic endocrine tumors. Clin Cancer Res 2008;14:6634–9.
19. Giatromanolaki A, Koukourakis MI, Pezzella F, et al. Expression of prolyl-hydroxylases PHD-1, 2 and 3 and of the asparagine hydroxylase FIH in non-small cell lung cancer relates to an activated HIF pathway. Cancer Lett 2008;262:87–93.
20. Tan EY, Campo L, Han C, et al. Cytoplasmic location of factor-inhibiting hypoxia-inducible factor is associated with an enhanced hypoxic response and a shorter survival in invasive breast cancer. Breast Cancer Res 2007;9:R89.
21. Bandres E, Cubedo E, Agirre X, et al. Identification by real-time PCR of 13 mature microRNAs differentially expressed in colorectal cancer and non-tumoral tissues. Mol Cancer 2006;5:29.
22. Slaby O, Svoboda M, Fabian P, et al. Altered expression of miR-21, miR-31, miR-143 and miR-145 is related to clinicopathologic features of colorectal cancer. Oncology 2007;72:397–402.
23. Volinia S, Calin GA, Liu CG, et al. A microRNA expression signature of human solid tumors defines cancer gene targets. Proc Natl Acad Sci U S A 2006;103:2257–61.
24. Wong QW, Lung RW, Law PT, et al. MicroRNA-223 is commonly repressed in hepatocellular carcinoma and potentiates expression of Stathmin1. Gastroenterology 2008;135:257–69.
25. Veerla S, Lindgren D, Kvist A, et al. MiRNA expression in urothelial carcinomas: important roles of miR-10a, miR-222, miR-125b, miR-7 and miR-452 for tumor stage and metastasis, and frequent homozygous losses of miR-31. Int J Cancer 2009;124:2236–42.
26. Yan LX, Huang XF, Shao Q, et al. MicroRNA miR-21 overexpression in human breast cancer is associated with advanced clinical stage, lymph node metastasis and patient poor prognosis. RNA 2008;14:2348–60.
27. Valastyan S, Reinhardt F, Benaich N, et al. A pleiotropically acting microRNA, miR-31, inhibits breast cancer metastasis. Cell 2009;137:1032–46.
28. Chen Y, Stallings RL. Differential patterns of microRNA expression in neuroblastoma are correlated with prognosis, differentiation, and apoptosis. Cancer Res 2007;67:976–83.
29. Chow TH, Lin YY, Hwang JJ, et al. Diagnostic and therapeutic evaluation of 111In-vinorelbine-liposomes in a human colorectal carcinoma HT-29/luc-bearing animal model. Nucl Med Biol 2008;35:623–34.
30. Lu SY, Chang KW, Liu CJ, et al. Ripe areca nut extract induces G1 phase arrests and senescence-associated phenotypes in normal human oral keratinocyte. Carcinogenesis 2006;27:1273–84.
31. Lu HH, Liu CJ, Liu TY, Kao SY, Lin SC, Chang KW. Areca-treated fibroblasts enhance tumorigenesis of oral epithelial cells. J Dent Res 2008;87:1069–74.
32. Tazawa H, Tsuchiya N, Izumiya M, Nakagama H. Tumor-suppressive miR-34a induces senescence-like growth arrest through modulation of the E2F pathway in human colon cancer cells. Proc Natl Acad Sci U S A 2007;104:15472–7.
33. Meng F, Henson R, Lang M, et al. Involvement of human micro-RNA in growth and response to chemotherapy in human cholangiocarcinoma cell lines. Gastroenterology 2006;130:2113–29.
34. Kulshreshtha R, Ferracin M, Wojcik SE, et al. A microRNA signature of hypoxia. Mol Cell Biol 2007;27:1859–67.
35. Taguchi A, Yanagisawa K, Tanaka M, et al. Identification of hypoxia-inducible factor-1 α as a novel target for miR-17-92 microRNA cluster. Cancer Res 2008;68:5540–5.
36. Fasanaro P, D'Alessandra Y, Di Stefano V, et al. MicroRNA-210 modulates endothelial cell response to hypoxia and inhibits the receptor tyrosine-kinase ligand Ephrin-A3. J Biol Chem 2008;383:15878–83.
37. van der Riet P, Nawroz H, Hruban RH, et al. Frequent loss of chromosome 9p21-22 early in head and neck cancer progression. Cancer Res 1994;54:1156–8.
38. Bertout JA, Patel SA, Simon MC. The impact of O_2 availability on human cancer. Nat Rev Cancer 2008;8:967–75.
39. Stolze IP, Tian YM, Appelhoff RJ, et al. Genetic analysis of the role of the asparaginyl hydroxylase factor inhibiting hypoxia-inducible factor (HIF) in regulating HIF transcriptional target genes. J Biol Chem 2004;279:42719–25.
40. Metzen E, Berchner-Pfannschmidt U, Stengel P, et al. Intracellular localisation of human HIF-1α hydroxylases: implications for oxygen sensing. J Cell Sci 2003;116:1319–26.